X-932-75-222

NASA TM X- 71057

# GRAVSAT/GEOPAUSE COVARIANCE ANALYSIS INCLUDING GEOPOTENTIAL ALIASING



DAVID W. KOCH


OCTOBER 1975

GSFC

GODDARD SPACE FLIGHT CENTER
GREENBELT, MARYLAND

Partially based upon material presented at the American Geophysical Union, Fall Annual Meeting, December 12-17, 1974, San Francisco, California

X-932-75-222

# GRAVSAT/GEOPAUSE COVARIANCE ANALYSIS INCLUDING GEOPOTENTIAL ALIASING

David W. Koch

October 1975

GODDARD SPACE FLIGHT CENTER
Greenbelt, Maryland

## CONTENTS



## ILLUSTRATIONS



## TABLES



*Uncertainties listed in Tables 5 through 8 are evaluated after the same tracking intervals.

TABLES (Contd.)

# GRAVSAT/GEOPAUSE COVARIANCE ANALYSIS INCLUDING GEOPOTENTIAL ALIASING

David W. Koch

## ABSTRACT

NASA's ongoing Earth and Ocean Dynamics Applications Program (EODAP) uses satellite technology and instrumentation to sense and monitor a wide range of natural phenomena. Among the proposed missions within this program is the GRAVSAT/GEOPAUSE which employs satellite-to-satellite tracking technology in an attempt to obtain improvements in the accuracies of the geopotential field and the global geoid. This report describes a conventional covariance analysis of that mission in which the uncertainties of approximately 200 parameters, including the geopotential coefficients to degree and order 12, are estimated over three different tracking intervals. The estimated orbital uncertainties for both GRAVSAT and GEOPAUSE reach levels more accurate than presently available. The adjusted measurement bias errors approach the mission goal. Survey errors in the low centimeter range are achieved after ten days of tracking. The ability of the mission to obtain accuracies of geopotential terms to (12, 12) one to two orders of magnitude superior to present accuracy levels is clearly shown. A unique feature of this report is that the aliasing structure of this (12, 12) field is examined. It is shown that uncertainties for unadjusted terms to (12, 12) still exert a degrading effect upon the adjusted error of an arbitrarily selected term of lower degree and order. Finally, the distribution of the aliasing from the unestimated uncertainty of a particular high degree and order geopotential term upon the errors of all remaining adjusted terms is listed in detail.

# GRAVSAT/GEOPAUSE COVARIANCE ANALYSIS INCLUDING GEOPOTENTIAL ALIASING

## EODAP AND GRAVSAT/GEOPAUSE

The Earth and Ocean Dynamics Program (EODAP) formerly EOPAP (Ref. 1), conceived and managed by NASA, applies sophisticated satellite technology to the continuous global sensing and monitoring of a wide range of diverse natural phenomena. Earth orbiting satellites, utilizing their complex onboard sensing instruments, provide the unprecedented capability for automated global data gathering. The EODAP program is specifically designed to exploit the inherent advantages of satellites and their instruments to achieve a better understanding of earth and ocean dynamics. Continuous and precise observations of the earth's various dynamic phenomena are necessary to develop the complex mathematical models of earthquakes. Accurate observations of the ocean's dynamics lead to increased understanding of the surface conditions and general ocean circulation. Such data can be utilized immediately by the shipping industry. It needs this data to plan ship routes which can take advantage of prevailing currents with attendant savings in both time and fuel. Indeed, it is difficult at present to foresee the full potential of this monitoring of natural phenomena by satellites.

Because of the variety and complexity of natural phenomena, the EODAP program necessarily involves many satellite missions, e.g. the GEOS-C, MAGSAT, SEASAT, GRAVSAT, and GEOPAUSE. GEOS-C employs a satellite-to-ocean radar altimeter with a one meter precision to determine the short-wavelength undulations of the ocean geoid to an equivalent vertical accuracy. SEASAT, a successor to GEOS-C, uses this same altimeter with a proposed 10 cm accuracy level to sense the sea surface, currents, and general ocean circulation. Such data will be used in the study of geoid undulations, wind stresses on surface water, location and mapping of boundary currents, and tides. GRAVSAT (Ref. 2) is a proposed low altitude (~300 km) surface force compensated satellite used with a companion satellite at the same height or with a high altitude satellite such as GEOPAUSE or possibly a tracking and data relay satellite (TDRS). GRAVSAT is an instrument which is expected to provide the means for a determination of the geopotential field to a 2.5° resolution and a global geoid to a 10 cm accuracy. An improved determination of the field will have an immediate beneficial impact. In satellite orbit determination, the geopotential inaccuracies are a well established error source, especially over long orbital arcs. As an

example, Ref. 3 describes the degrading effect of these inaccuracies upon a multi-revolution GEOS-C orbit. Satellite tracking and the subsequent data processing could be performed more efficiently and economically with a more accurate field, since in a given situation less data would have to be processed to determine an orbit.

GEOPAUSE (Ref. 4) is a high altitude tracking relay spacecraft in a precisely determined orbit. Data from this satellite is expected to determine the orbits of lower satellites such as SEASAT and GRAVSAT to a 10 cm accuracy and also to establish the position and dynamics of points on the earth's surface. The latter includes determination of polar motion, earth rotation, tectonic plate motion, and solid earth tides. Furthermore, the data may also be used to estimate both reference station locations and radio tracking instrument biases to the centimeter level.

The basic GEOPAUSE satellite system concept has been investigated previously by Siry (Ref. 5). Therein he describes the potential contributions and characteristics of such a system. In addition, the utility of the system in geodynamics and global surveys of natural phenomena is discussed. Another report by Koch and Argentiero (Ref. 6) documented an initial mission analysis study of the combined GRAVSAT/GEOPAUSE concept oriented toward low degree and order geopotential uncertainty recovery. That particular report demonstrated that data from GRAVSAT/GEOPAUSE could be used to determine uncertainties in the spherical harmonic coefficients of the geopotential field from (0, 0) through (8, 6) inclusive to an accuracy one to two orders of magnitude over current levels. This present report follows and expands upon that study. In the present report the uncertainties of a larger (12, 12) field are recovered, additional perturbative forces are considered, and parameters such as survey errors and instrument biases are estimated. An important matter, usually not investigated, is the aliasing structure of such a larger geopotential field. The aliasing effect of the uncertainties of unadjusted geopotential terms upon the error of an arbitrarily selected adjusted term is considered herein. The present report also stresses the difference, if any, between uncertainties of various parameters when the tracking interval is varied over three, six, and ten days.

## THE GRAVSAT/GEOPAUSE MISSION

**The proposed GRAVSAT/GEOPAUSE mission involves satellite-to-satellite tracking technology combined with a unique orbital geometry in an attempt to obtain improvements in the accuracies of the geopotential field and global geoid. Table 1 lists, in a general context, the rationale, description, and the applicability of the results for such a mission.**

Table 1
The GRAVSAT/GEOPAUSE Mission

I. RATIONALE

**The present uncertainties in the geopotential field are a fundamental error source in earth and ocean physics. Meeting stringent EODAP objectives will require a new approach to estimation of these accuracies.**

II. DESCRIPTION

**Hi-lo satellite-to-satellite tracking data used to extract field coefficients from low satellite orbital perturbations.**

(1) GRAVSAT
Low altitude surface force compensated satellite

(2) GEOPAUSE
High altitude tracking relay satellite.

III. APPLICABILITY OF RESULTS

More accurate geopotential field leads to improvements in:

(1) Orbit determination and prediction
(2) Satellite data processing
(3) Accuracy of earth and marine geoid.

The overall geometry of the mission is depicted in Figure 1. The mission involves a low GRAVSAT and a high GEOPAUSE satellite in coplanar, polar, and circular orbits. Their common orbital plane is normal to both the ecliptic and equatorial planes. The perpendicularity of the plane to the ecliptic minimizes long term luni-solar perturbations upon the plane, thus insuring long term orbital stability. A polar orbit guarantees complete sampling of the earth's gravity field by GRAVSAT. Geopotential coefficients from such a global sample will achieve orthogonality and will not be degraded by aliasing or poor statistical independence. The orbit of the high GEOPAUSE is minimally perturbed by existing inaccuracies in the gravity field. Consequently GEOPAUSE can function as a

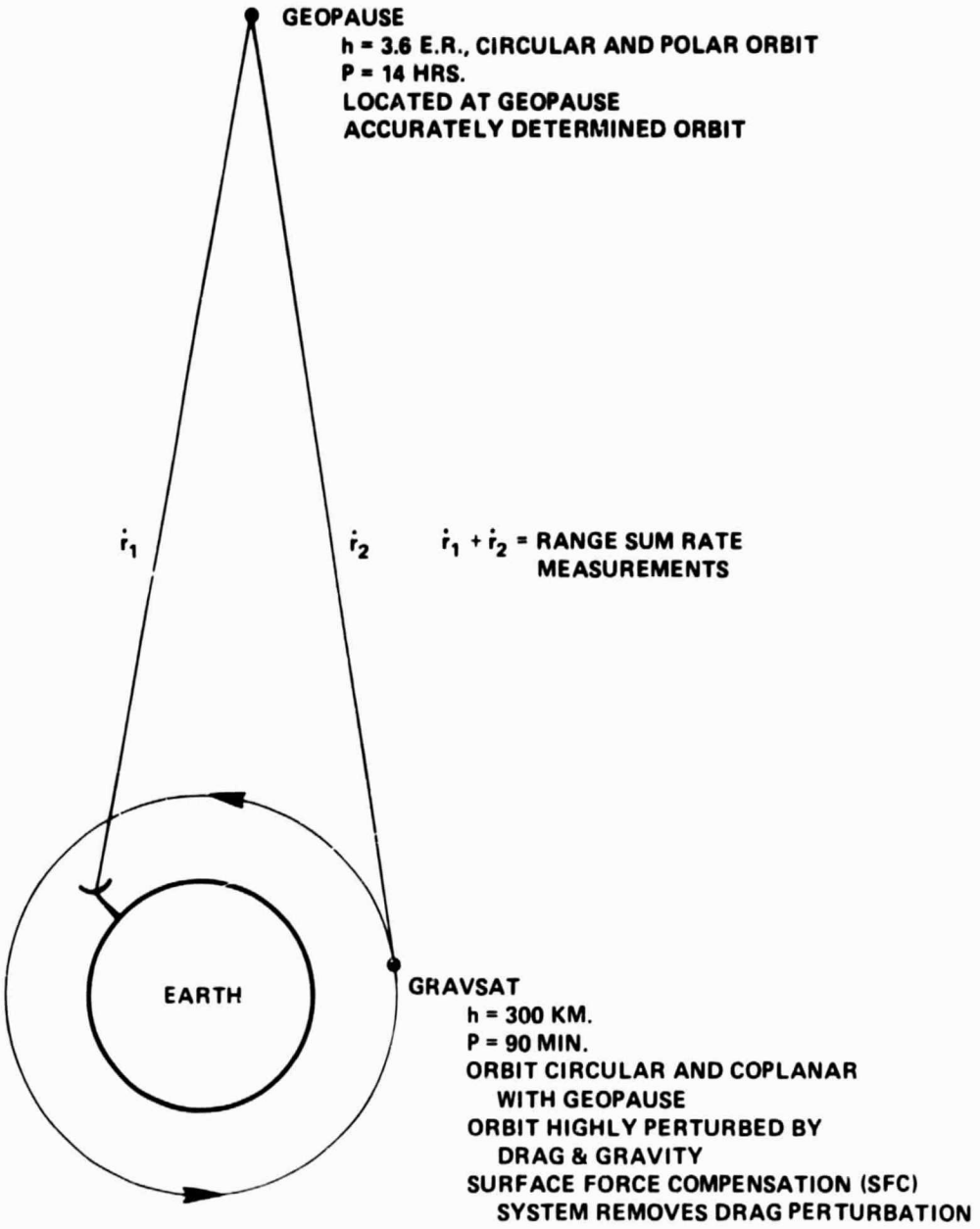


Figure 1. GRAVSAT/GEOPAUSE Geometry

stable high altitude relay tracking station. The GRAVSAT orbit at a height of only 300 km will be highly perturbed by external forces, principally atmospheric drag and gravitational uncertainties, and to a lesser extent by implementation of surface force compensation (SFC). Two difficulties immediately arise. First, the orbital perturbations due to external forces must be separated as to their origin. Second, the perturbations due to implementation of SFC must be properly treated so that any lack of knowledge of this self gravitational force will not degrade the remaining estimates.

The first difficulty is overcome by the unique construction of the actual GRAVSAT spacecraft combined with an onboard SFC. The spacecraft will consist of two concentric spheres. The outer sphere experiences perturbations caused by both gravitational and non-gravitational forces whereas the inner experiences solely the former. This imbalance of forces causes the outer sphere to be progressively displaced toward the inner as the GRAVSAT proceeds in orbit. The sensitive instrumentation of the SFC system will sense such a displacement. When this displacement exceeds a prescribed distance, the SFC system actuates jets on the exterior of the outer sphere until both spheres are concentric again. Meanwhile, during the entire displacement and repositioning, the inner sphere has followed an orbit perturbed solely by gravity. Thus the SFC essentially has nullified the orbital perturbations due to non-gravitational forces and has constrained both spheres of the GRAVSAT to follow an orbit perturbed solely by gravity. It is these orbital perturbations, caused only by gravity, that the tracking system senses and from which gravity coefficient estimates can be extracted.

The second difficulty involves the proper statistical treatment of the force caused by the mutual attraction between the masses of the inner and outer spheres of the GRAVSAT. This force is assumed constant of unknown magnitude and acting solely in the along track direction opposite to the direction of the velocity vector. Therefore, it can be treated as a standard differential correction type bias and its uncertainty estimated.

A tracking network of six ground stations was chosen to track GRAVSAT through GEOPAUSE. Three properly placed stations in each hemisphere provide continuous coverage of GEOPAUSE by at least one station. Such coverage insures no permanent spatial gaps in the sampling of the gravity field by GRAVSAT. Each station measures range sum rate with a one minute integration time over a ten day data interval. This interval constitutes one complete sampling of the gravity field by GRAVSAT.

The nominal mission parameters follow:

(1) ORBITS

Epoch: July 1, 1979, $0^H$, UT
Geocentric True Earth Equator and Equinox of Date

| | GRAVSAT | GEOPAUSE |
|---|---|---|
| a(km)* | 6,678.133 | 29,431.213 |
| e | 0.0 | 0.0 |
| i(deg) | 90.0 | 90.0 |
| $\Omega$ (deg) | 90.0 | 90.0 |
| $\omega$ (deg) | 180.0 | 180.0 |
| M(deg) | 180.0 | 180.0 |
| h(km) | 300.0 | 23,053.190(3.6 E.R.) |
| P(hrs) | 1.5 | 14.0 |

(2) TRACKING STATIONS

Northern Hemisphere: Guam, Madrid, and Rosman
Southern Hemisphere: Canberra, Johannesburg, and Santiago

(3) MEASUREMENTS AND UNCERTAINTIES

Range sum rate measurements every minute over ten days with random 0.2 mm/sec noise and fixed ±1 mm/sec bias.

(4) ESTIMATED PARAMETERS

| NAME | DIMENSION |
|---|---|
| GRAVSAT epoch state | 6 |
| GEOPAUSE epoch state | 6 |
| Range sum rate bias | 6 |
| Station survey components | 15 |
| Residual force upon GRAVSAT | 1 |
| Sine and cosine components of spherical harmonic expansion of geopotential field through (12, 12) | 165 |

*a through M are orbital elements; a is the semi-major axis, e is the eccentricity, i is the inclination, $\Omega$ is the right ascension, $\omega$ is the argument of perigee, and M is the mean anomaly; h and P are the orbital height and period, respectively.

## RESULTS

Under the previous assumptions, a covariance analysis simulation was performed using the NAP parameter estimation/NAPCOV covariance analysis computer programs (Ref. 9-12). Instead of performing an actual least squares reduction of simulated or real data, the simulation derived only the covariance matrix of such a process. Furthermore, the simulation assumed that perturbations in the data are linearly related to the perturbations of the systematic and dynamic error sources under consideration. The uncertainties for all parameters were estimated simultaneously. Solving for all parameters together should theoretically minimize the uncertainties of their estimates. However, this approach ignores the effect of the uncertainties of the unadjusted parameters upon the errors of the estimated ones (aliasing) and consequently may give optimistic results.

Tables 2 through 6 list the a priori and a posteriori uncertainties after the processing of three, six, and ten days of tracking data for all the parameters estimated during the numerical simulation. For convenience, both the individual and RSS* uncertainties for groups of parameters are listed where applicable. The correlation matrix between the GRAVSAT and GEOPAUSE epoch states after ten days of tracking is also listed. The first two tables concentrate on the adjusted errors of the GRAVSAT and GEOPAUSE epoch states and their associated correlation structure. Table 2 indicates a substantial overall reduction in uncertainties of each component of both state vectors from their rather conservative a priori values. This reduction of uncertainties demonstrates the ability of the GEOPAUSE to act as a tracking relay spacecraft for use in recovering low satellite orbits. For the GRAVSAT orbit the largest uncertainties are predictably out-of-plane (x direction). Since their two orbits are coplanar, GEOPAUSE can sense only in-plane (y and z directions) GRAVSAT orbital perturbations and hence no out-of-plane information about the GRAVSAT orbit is obtained. However, with increased tracking data even these out-of- plane errors tend to decrease. The a posteriori RSS position uncertainties drop approximately linearly with time whereas the corresponding velocity errors drop by a factor of approximately twenty percent between tracking intervals and eventually reach the 2 mm/s level at 10 days. Both position and velocity adjusted RSS uncertainties are almost entirely composed of out-of-plane errors. The remaining estimated in-plane uncertainties are relatively insensitive to additional tracking.

For the GEOPAUSE orbit, the out-of-plane and one in-plane (z direction) a posteriori position uncertainties behave in a similar manner. Both decrease slowly and eventually reach a level of about 65 cm after ten days of tracking. The adjusted error of the remaining position component remains essentially constant. The adjusted RSS position uncertainty decreases uniformly from 2.11 meters after three days of tracking to below the meter level after ten days. The adjusted RSS velocity uncertainties remain below 0.25 mm/s throughout. According to

*RSS is the square root of the sum of the squares.

3, 6, and 10 Days of Tracking

| Epoch States | | A Priori Uncertainty | A Posteriori Uncertainty | | |
|---|---|---|---|---|---|
| | | | 3 Days | 6 Days | 10 Days |
| GRAVSAT | X (m) | 200 | 16.66 | 8.14 | 4.78 |
| | Y (m) | 200 | .04 | .02 | .02 |
| | Z (m) | 200 | .35 | .20 | .14 |
| | RSS (m) | 346 | 16.66 | 8.14 | 4.78 |
| | $\dot{X}$ (mm/s) | 200 | 72.25 | 13.32 | 2.36 |
| | $\dot{Y}$ (mm/s) | 200 | .41 | .23 | .17 |
| | $\dot{Z}$ (mm/s) | 200 | .07 | .04 | .03 |
| | RSS (mm/s) | 346 | 72.25 | 13.32 | 2.37 |
| GEOPAUSE | X (m) | 150 | 1.43 | .89 | .65 |
| | Y (m) | 150 | .07 | .04 | .03 |
| | Z (m) | 150 | 1.55 | .87 | .62 |
| | RSS (m) | 260 | 2.11 | 1.25 | .90 |
| | $\dot{X}$ (mm/s) | 150 | .13 | .07 | .05 |
| | $\dot{Y}$ (mm/s) | 150 | .19 | .11 | .08 |
| | $\dot{Z}$ (mm/s) | 150 | .01 | .00 | .00 |
| | RSS (mm/s) | 260 | .23 | .13 | .09 |

published literature the present state-of-the-art orbital position uncertainty is approximately 10 meters. Results indicate that data from GEOPAUSE tracking GRAVSAT can be processed to achieve such an orbital accuracy within six days.

Table 3 lists the symmetric correlation matrix between the GRAVSAT and GEOPAUSE epoch states after ten days of tracking. In general, the correlations reveal a good separability between estimates which is reflected in the a posteriori uncertainties of the previous table. The correlation coefficients conveniently separate into two distinct classes. The first consists of correlations with absolute values greater than 0.94 and the second with values less than 0.43. The correlation coefficients of large absolute value are circled within the table. These high correlations portend possible convergence problems during any future processing of real data from the mission. The highly correlated parameters are the Z and $\dot{Y}$ components from either state and GEOPAUSE Y with $\dot{Z}$. Indeed, two of these pairs, GEOPAUSE Y with $\dot{Z}$ and GEOPAUSE Z with $\dot{Y}$ have correlations with absolute value near unity. All remaining pairs of parameters are relatively weakly correlated.

Table 3

Correlation Matrix of GRAVSAT and GEOPAUSE States After 10 Days of Tracking

| | | GRAVSAT | | | | | | GEOPAUSE | | | | | |
|---|---|---|---|---|---|---|---|---|---|---|---|---|---|
| | | X | Y | Z | $\dot{X}$ | $\dot{Y}$ | $\dot{Z}$ | X | Y | Z | $\dot{X}$ | $\dot{Y}$ | $\dot{Z}$ |
| GRAVSAT | X | 1.00 | .03 | -.13 | .42 | .13 | -.04 | -.06 | .02 | -.14 | -.13 | .14 | -.02 |
| | Y | | 1.00 | -.02 | .09 | .03 | -.16 | -.05 | .22 | -.03 | -.03 | .03 | -.22 |
| | Z | | | 1.00 | -.18 | (-.95) | .00 | -.42 | .03 | (.97) | .08 | (-.97) | -.01 |
| | $\dot{X}$ | | | | 1.00 | .17 | -.06 | -.03 | -.10 | -.14 | .00 | .15 | .09 |
| | $\dot{Y}$ | | | | | 1.00 | .01 | .42 | -.03 | (-.95) | -.09 | (.95) | .02 |
| | $\dot{Z}$ | | | | | | 1.00 | .04 | -.14 | .02 | .02 | -.02 | .14 |
| GEOPAUSE | X | | | | | | | 1.00 | -.01 | -.41 | -.00 | .41 | .01 |
| | Y | | SYMMETRIC | | | | | | 1.00 | .03 | -.06 | -.03 | (.99) |
| | Z | | | | | | | | | 1.00 | .07 | (-.99) | -.00 |
| | $\dot{X}$ | | | | | | | | | | 1.00 | -.07 | .04 |
| | $\dot{Y}$ | | | | | | | | | | | 1.00 | .00 |
| | $\dot{Z}$ | | | | | | | | | | | | 1.00 |

Tables 4 and 5 depict the initial and adjusted errors for the range sum rate biases for six stations and the survey errors for five. No survey errors were computed for the sixth station due to program dimension limitations. The established measurement accuracy goal of .003 cm/sec is met by half of the stations after only three days of tracking and exceeded by all thereafter. Table 5 reveals that data from the GRAVSAT/GEOPAUSE combination can be used to recover survey errors with centimeter accuracy. Recovered RSS position uncertainties for all five stations decrease from approximately 60 cm to 30 and 20 cm after 3, 6, and 10 days of tracking, respectively. The present survey accuracy levels are in the low meter range. Thus significant improvements from the present accuracy level appear possible.

An independent analysis was conducted to determine the perturbations induced by geopotential uncertainties in the range sum rate data between a geosynchronous and GRAVSAT satellite. Perturbations in the data caused by the difference between nominal and actual geopotential values averaged more than 1 mm/sec. To satisfy GRAVSAT SFC requirements the ratio of the above perturbation to the perturbation caused by the unmodeled residual force should be approximately 10. Consequently, this force should cause a maximum data perturbation of 0.1 mm/sec. This corresponds to at most $10^{-8}$ g* uncertainty for the unmodeled force. Table 6 reveals that after three days of tracking an uncertainty of $10^{-10}$ g is reached and it decreases an order of magnitude for each additional tracking interval. Thus the requirement is achieved.

*g = 980 cm $sec^{-2}$, the earth's equatorial acceleration of gravity.

Table 4
Uncertainties of Range Sum Rate Measurement Biases
After 3, 6, and 10 Days of Tracking

| Station | A Priori Uncertainty (mm/s) | A Posteriori Uncertainty (mm/s) | | |
|---|---|---|---|---|
| | | 3 Days | 6 Days | 10 Days |
| Guam | 1.00 | .04 | .02 | .01 |
| Madrid | 1.00 | .04 | .02 | .01 |
| Rosman | 1.00 | .03 | .02 | .01 |
| Canberra | 1.00 | .04 | .02 | .01 |
| Johannesburg | 1.00 | .03 | .02 | .01 |
| Santiago | 1.00 | .03 | .02 | .01 |

Table 5
Station Survey Uncertainties After 3, 6, and 10 Days of Tracking

| Station | Survey Component | A Priori Uncertainty (m) | A Posteriori Uncertainty (cm) | | |
|---|---|---|---|---|---|
| | | | 3 Days | 6 Days | 10 Days |
| Guam | E* | 10.0 | 64.2 | 29.1 | 19.3 |
| | N | 10.0 | 30.4 | 13.1 | 9.4 |
| | V | 10.0 | 21.1 | 12.2 | 9.5 |
| | RSS | 17.3 | 74.1 | 34.2 | 23.5 |
| Madrid | E | 10.0 | 28.0 | 17.4 | 13.7 |
| | N | 10.0 | 45.8 | 16.9 | 12.7 |
| | V | 10.0 | 27.7 | 14.2 | 9.4 |
| | RSS | 17.3 | 60.4 | 28.1 | 20.9 |
| Rosman | E | 10.0 | 32.7 | 17.7 | 13.8 |
| | N | 10.0 | 18.2 | 9.9 | 7.8 |
| | V | 10.0 | 61.3 | 16.5 | 11.6 |
| | RSS | 17.3 | 71.8 | 26.1 | 19.6 |
| Canberra | E | 10.0 | 50.2 | 24.6 | 15.7 |
| | N | 10.0 | 22.8 | 16.2 | 10.9 |
| | V | 10.0 | 26.0 | 14.7 | 10.2 |
| | RSS | 17.3 | 61.0 | 32.9 | 21.7 |
| Johannesburg | E | 10.0 | 34.3 | 20.6 | 15.6 |
| | N | 10.0 | 18.1 | 10.5 | 7.5 |
| | V | 10.0 | 32.4 | 20.7 | 13.2 |
| | RSS | 17.3 | 50.5 | 31.0 | 21.8 |

*E, N, V are the station centered orthogonal east, north and vertical components, respectively, of the station survey error.

Table 6
Uncertainty of Residual Force Upon GRAVSAT After 3, 6 and 10 Days of Tracking

| Parameter | A Priori Uncertainty | A Posteriori Uncertainty | | |
|---|---|---|---|---|
| | | 3 Days | 6 Days | 10 Days |
| Unmodeled Residual Force Upon GRAVSAT (g) | $10^{-6}$ | $10^{-10}$ | $10^{-11}$ | $10^{-12}$ |

In (7) the coefficients of a harmonic expansion of the Goddard Earth Model-5 (GEM-5) geopotential field were calibrated against actual data of 15° × 15° gravity anomalies. The nominal covariance matrix was then scaled to be consistent with the residuals. The resulting normalized uncertainties ($\sigma_n$) from this matrix are displayed in Fig. 2 as percentages of Kaula's rule $s_n = 10^{-5}/n^2$, where n is the degree of the coefficient. This is an empirical formula which estimates the magnitude of normalized harmonic coefficients. These uncertainties increase exponentially from 5 to 60% through degree 12, thereafter all coefficients are uncertain to between 60% and 100% of their actual values. These large uncertainties are indicative of the severe aliasing and poor statistical independence inherent in the data from which these geopotential coefficients were estimated. These conditions are caused primarily by incomplete sampling of the gravity field. The orbit of GRAVSAT is specifically designed to obtain a total sample of the field. Such a sample should allow the coefficients to achieve orthogonality, thereby minimizing aliasing and dependence between coefficients.

Tables 7 and 8 give the improvement factors for the uncertainties of the sine and cosine terms of the geopotential coefficients. Improvement factors are the ratio of the a priori uncertainty as shown in Figure 2 divided by the uncertainty obtained during the simulation. Thus a factor of 100 represents an improvement in accuracy two orders of magnitude superior to present accuracy levels. It is clear there is at least one and sometimes a two order of magnitude improvement in the accuracy for all terms through (12, 12). Furthermore, there is only minimal improvement in the accuracy for most terms between different tracking intervals. Consequently, if accuracy improvement of geopotential terms were to become the objective of the GRAVSAT/GEOPAUSE mission, three days of continuous tracking apparently suffices.

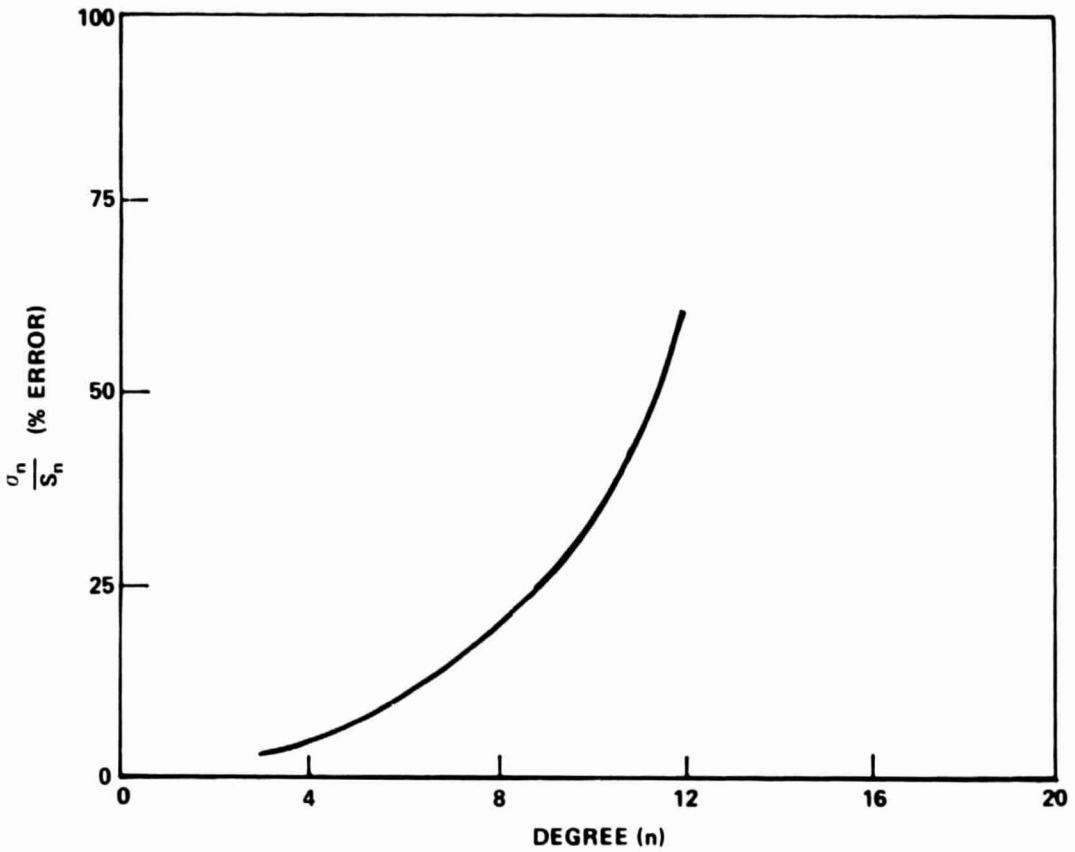


Figure 2. Present Uncertainty of Low Order Geopotential Coefficients

Table 7

Improvement Factor of the Uncertainties in Sine Term of Geopotential Coefficients After 3, 6, and 10 Days of Tracking

| Degree | Order | Tracking Interval | | | Degree | Order | Tracking Interval | | | Degree | Order | Tracking Interval | | | Degree | Order | Tracking Interval | | |
|---|---|---|---|---|---|---|---|---|---|---|---|---|---|---|---|---|---|---|---|
| n | m | 3 Days | 6 Days | 10 Days | n | m | 3 Days | 6 Days | 10 Days | n | m | 3 Days | 6 Days | 10 Days | n | m | 3 Days | 6 Days | 10 Days |
| 2 | 1 | 117 | 172 | 226 | 6 | 6 | 37 | 63 | 84 | 9 | 4 | 37 | 53 | 68 | 11 | 4 | 43 | 60 | 78 |
| | 2 | 95 | 171 | 228 | 7 | 1 | 32 | 44 | 58 | | 5 | 36 | 54 | 69 | | 5 | 39 | 57 | 73 |
| 3 | 1 | 72 | 104 | 135 | | 2 | 32 | 44 | 57 | | 6 | 36 | 56 | 73 | | 6 | 46 | 65 | 86 |
| | 2 | 54 | 75 | 98 | | 3 | 32 | 43 | 57 | | 7 | 27 | 56 | 74 | | 7 | 26 | 58 | 75 |
| | 3 | 72 | 106 | 141 | | 4 | 32 | 46 | 60 | | 8 | 36 | 65 | 87 | | 8 | 42 | 77 | 106 |
| 4 | 1 | 34 | 48 | 62 | | 5 | 26 | 49 | 63 | | 9 | 56 | 105 | 136 | | 9 | 38 | 72 | 94 |
| | 2 | 32 | 47 | 61 | | 6 | 32 | 51 | 68 | 10 | 1 | 33 | 46 | 60 | | 10 | 99 | 250 | 402 |
| | 3 | 27 | 40 | 56 | | 7 | 31 | 76 | 101 | | 2 | 34 | 46 | 60 | | 11 | 376 | 648 | 915 |
| | 4 | 35 | 59 | 78 | 8 | 1 | 32 | 44 | 57 | | 3 | 34 | 46 | 60 | 12 | 1 | 38 | 53 | 68 |
| 5 | 1 | 44 | 62 | 81 | | 2 | 32 | 43 | 56 | | 4 | 34 | 47 | 61 | | 2 | 41 | 56 | 72 |
| | 2 | 44 | 60 | 79 | | 3 | 32 | 43 | 57 | | 5 | 33 | 50 | 63 | | 3 | 39 | 53 | 68 |
| | 3 | 43 | 60 | 80 | | 4 | 30 | 44 | 58 | | 6 | 32 | 49 | 64 | | 4 | 41 | 58 | 75 |
| | 4 | 42 | 63 | 83 | | 5 | 27 | 47 | 61 | | 7 | 24 | 50 | 65 | | 5 | 40 | 57 | 72 |
| | 5 | 53 | 94 | 124 | | 6 | 30 | 48 | 63 | | 8 | 30 | 53 | 71 | | 6 | 41 | 60 | 78 |
| 6 | 1 | 29 | 41 | 54 | | 7 | 25 | 50 | 68 | | 9 | 36 | 65 | 83 | | 7 | 30 | 58 | 74 |
| | 2 | 29 | 40 | 52 | | 8 | 45 | 81 | 110 | | 10 | 66 | 113 | 150 | | 8 | 37 | 66 | 88 |
| | 3 | 28 | 40 | 53 | 9 | 1 | 36 | 51 | 66 | 11 | 1 | 38 | 53 | 69 | | 9 | 41 | 70 | 92 |
| | 4 | 26 | 43 | 56 | | 2 | 37 | 51 | 66 | | 2 | 42 | 58 | 74 | | 10 | 50 | 91 | 122 |
| | 5 | 26 | 44 | 57 | | 3 | 37 | 50 | 65 | | 3 | 38 | 53 | 68 | | 11 | 94 | 157 | 210 |
| | | | | | | | | | | | | | | | | 12 | 421 | 965 | 1,379 |

$$\text{Improvement Factor} = \frac{\text{A Priori Uncertainty}}{\text{A Posteriori Uncertainty}}$$

Table 8

Improvement Factor of the Uncertainties in Cosine Term of Geopotential Coefficients After 3, 6, and 10 Days of Tracking

| n Degree | m Order | Tracking Interval | | | n Degree | m Order | Tracking Interval | | | n Degree | m Order | Tracking Interval | | | n Degree | m Order | Tracking Interval | | |
|---|---|---|---|---|---|---|---|---|---|---|---|---|---|---|---|---|---|---|---|
| | | 3 Days | 6 Days | 10 Days | | | 3 Days | 6 Days | 10 Days | | | 3 Days | 6 Days | 10 Days | | | 3 Days | 6 Days | 10 Days |
| 2 | 0 | 189 | 289 | 373 | 6 | 4 | 27 | 42 | 55 | 9 | 2 | 37 | 52 | 66 | 11 | 3 | 38 | 54 | 69 |
| | 1 | 115 | 170 | 218 | | 5 | 25 | 40 | 56 | | 3 | 36 | 51 | 66 | | 4 | 42 | 60 | 78 |
| | 2 | 106 | 173 | 233 | | 6 | 36 | 62 | 84 | | 4 | 38 | 52 | 68 | | 5 | 38 | 54 | 71 |
| 3 | 0 | 90 | 127 | 168 | 7 | 0 | 46 | 63 | 82 | | 5 | 35 | 50 | 67 | | 6 | 43 | 65 | 86 |
| | 1 | 73 | 103 | 131 | | 1 | 32 | 44 | 56 | | 6 | 32 | 55 | 74 | | 7 | 44 | 60 | 81 |
| | 2 | 53 | 76 | 98 | | 2 | 31 | 45 | 58 | | 7 | 45 | 59 | 80 | | 8 | 44 | 83 | 111 |
| | 3 | 72 | 110 | 143 | | 3 | 31 | 45 | 58 | | 8 | 38 | 68 | 91 | | 9 | 38 | 68 | 97 |
| 4 | 0 | 49 | 69 | 88 | | 4 | 32 | 46 | 60 | | 9 | 56 | 99 | 140 | | 10 | 100 | 241 | 388 |
| | 1 | 34 | 47 | 60 | | 5 | 28 | 45 | 61 | 10 | 0 | 48 | 66 | 85 | | 11 | 366 | 704 | 959 |
| | 2 | 33 | 48 | 62 | | 6 | 28 | 51 | 69 | | 1 | 34 | 46 | 58 | 12 | 0 | 57 | 80 | 103 |
| | 3 | 26 | 42 | 56 | | 7 | 54 | 80 | 109 | | 2 | 33 | 47 | 60 | | 1 | 38 | 52 | 65 |
| | 4 | 36 | 57 | 77 | 8 | 0 | 45 | 62 | 80 | | 3 | 33 | 47 | 60 | | 2 | 40 | 57 | 73 |
| 5 | 0 | 62 | 87 | 114 | | 1 | 32 | 44 | 55 | | 4 | 34 | 47 | 61 | | 3 | 38 | 54 | 69 |
| | 1 | 44 | 62 | 78 | | 2 | 31 | 44 | 57 | | 5 | 33 | 46 | 61 | | 4 | 41 | 58 | 74 |
| | 2 | 43 | 62 | 79 | | 3 | 31 | 45 | 57 | | 6 | 28 | 49 | 64 | | 5 | 39 | 54 | 70 |
| | 3 | 41 | 62 | 80 | | 4 | 31 | 44 | 57 | | 7 | 39 | 52 | 70 | | 6 | 40 | 60 | 78 |
| | 4 | 42 | 62 | 82 | | 5 | 27 | 44 | 59 | | 8 | 33 | 56 | 75 | | 7 | 45 | 60 | 80 |
| | 5 | 55 | 89 | 121 | | 6 | 26 | 48 | 64 | | 9 | 35 | 61 | 86 | | 8 | 40 | 69 | 91 |
| 6 | 0 | 42 | 59 | 75 | | 7 | 39 | 54 | 73 | | 10 | 64 | 108 | 148 | | 9 | 37 | 67 | 93 |
| | 1 | 30 | 41 | 52 | | 8 | 48 | 85 | 114 | 11 | 0 | 60 | 85 | 119 | | 10 | 49 | 87 | 120 |
| | 2 | 29 | 41 | 53 | 9 | 0 | 53 | 73 | 93 | | 1 | 39 | 53 | 66 | | 11 | 99 | 163 | 212 |
| | 3 | 27 | 41 | 53 | | 1 | 37 | 51 | 64 | | 2 | 41 | 58 | 75 | | 12 | 396 | 896 | 1,339 |

$$\text{Improvement Factor} = \frac{\text{A Priori Uncertainty}}{\text{A Posteriori Uncertainty}}$$

## GEOPOTENTIAL ALIASING

The geopotential field is representable by an infinite series of spherical harmonic terms. Estimating the field consists of solving for both the sine and cosine coefficients of these spherical harmonics. Since it is obviously impossible to estimate an infinite number of coefficients, this series is usually truncated at some term and all terms thereafter are set equal to zero or assumed perfectly known at some nominal value. Since neither is strictly true, the truncation invariably introduces an error upon the terms to be estimated which precede the point of truncation. This mismodeling error is called "aliasing" and is indeed the dominant problem in geopotential estimation. As an example of this aliasing phenomenon, consider the following simple example. A natural phenomenon is modeled correctly by the quadratic $y = x^2 + x + 1$. A researcher, however, assumes that the linear equation $y = ax + b$ correctly models it. This assumed model neglects the second degree term of the correct model, in effect equating it to zero. Next he performs a standard least squares fit to the three data points $y(0) = 1$, $y(5) = 31$, and $y(10) = 111$ using the linear model. He determines $y = 11x - 7.33$ best fits the data. The estimated coefficients of fit are $a = 11$ and $b = -7.33$ whereas the correct values are $a = b = 1$. Thus neglecting the second degree term in the correct model has seriously degraded the quality of the estimates from the least squares fit. This degradation is an example of the "aliasing". This same aliasing exists on a much larger scale in geopotential coefficient estimation. The neglect of the uncertainties of the high degree and order unestimated coefficients aliases the error of the remaining estimated coefficients. A mathematically rigorous description of this aliasing and orthogonality properties of geopotential coefficients is developed by Argentiero and Garza-Robles (Ref. 8).

During a covariance analysis each parameter under investigation is placed in either an "estimated" or "consider" category. The former contains those parameters which ordinarily would be solved for during an actual orbit determination process, e.g. satellite state or instrument biases. The latter includes parameters which would remain unestimated during such a process but whose uncertainties are taken into account in computing the covariance matrix of the process. Measurement timing and atmospheric refraction are typical consider parameters. The software (Ref. 9-12) used during this study conveniently separates the variance of each "estimated" parameter into a series of variances due to the individual "consider" parameters and the variance due to the data noise. The error contribution of a specific "consider" parameter to the error of an "estimated" parameter is called its "aliasing."

As mentioned previously, results to date neglect the aliasing phenomenon introduced by the uncertainties of the unadjusted parameters and thus tend to be somewhat optimistic. To obtain some quantitative measure of this aliasing, the

covariance analysis was reconsidered using two different estimation strategies. The first strategy attempts to determine the aliasing impact upon the uncertainty of a centrally located adjusted geopotential term of low degree and order due to the uncertainties of the surrounding unadjusted terms. Consequently, the uncertainties of both satellite epoch states, measurement biases, station survey components, unmodeled residual force, and an arbitrarily selected geopotential term, C(5, 2), were placed in the "estimated" category. The uncertainties of the remaining 164 geopotential terms surrounding C(5, 2) were placed in the "consider" mode. Such a strategy reveals, at least for one particular term, the degrading influence of the remaining terms and would identify those particular ones with the greatest aliasing. Alias maps for all terms should be estimated for the total aliasing effect. However, an alias map for one term gives at least some insight to the aliasing problem. The aliasing effect of the uncertainties of the unadjusted terms upon the error of C(5, 2) is displayed in Table 9 as an alias map for C(5, 2). The unnormalized a priori uncertainty ($\sigma_0$) of C(5, 2) as determined from Figure 2 is $10^{-8}$. The adjusted uncertainty ($\hat{\sigma}$) was $10^{-7}$. In general, two results are immediately obvious. First, the uncertainties of all the surrounding terms alias the adjusted error of C(5, 2) to varying degrees. Second there is wide variation in the magnitude of this aliasing. This second factor is of special importance since it indicates which particular geopotential terms should be estimated concurrently with C(5, 2) to minimize the overall degrading influence of aliasing. At least to the degree and order considered in the alias map, an interesting pattern immediately emerges. The surrounding terms of odd degree and even order to order 4 exhibit markedly higher aliasing upon C(5, 2) than the remaining terms. The contributions of these particular terms are boxed twice within Table 9. The magnitudes of the aliasing for these terms is greatest for the lowest order and decreases rapidly within a degree reaching approximately 2 or $3 \times 10^{-10}$ RSS[1] aliasing at order 4. Within an order, the aliasing increases slightly with increasing degree. Indeed, term (11, 0) alone contributes $182.4 \times 10^{-10}$ in an RSS sense to the adjusted uncertainty of $10^{-7}$ for C(5, 2). Thus the odd degree zonals are seen to contribute the maximum aliasing upon C(5, 2) and therefore should be estimated simultaneously with C(5, 2). All the remaining terms contribute much less aliasing and could remain in the consider mode.

The second strategy investigates the extent and magnitude of aliasing induced by an unestimated high degree and order geopotential term upon terms of lower degree and order. The covariance analysis was reconsidered with only the uncertainty of C(12, 6) in the consider mode and all remaining uncertainties estimated. C(12, 6) has an initial uncertainty of $10^{-13}$. The information obtained by such a strategy is important because it determines how much of tne

(1) RSS of sine and cosine components of the geopotential term.

Table 9

Alias Map for C(5, 2)

RSS Aliasing Contributions $\times 10^{10}$ to the Uncertainty of C(5, 2) Due to the Uncertainties of Surrounding Unestimated Coefficients After 10 Days of Tracking

| Degree (N) \ Order (M) | 0 | 1 | 2 | 3 | 4 | 5 | 6 | 7 | 8 | 9 | 10 | 11 | 12 |
|---|---|---|---|---|---|---|---|---|---|---|---|---|---|
| 2 | .689 | .146 | 2.86 | | | | | | | | | | |
| 3 | 144.0 | .391 | 57.8 | 1.13 | | | | | | | | | |
| 4 | .197 | .029 | .662 | .110 | 1.61 | | | | | | | | |
| 5 | 148.6 | .291 | $\sigma_0 = 10^{-8}$ $\hat{\sigma} = 10^{-7}$ | .848 | 2.13 | .911 | | | | | | | |
| 6 | .147 | .223 | .629 | .104 | 1.28 | .115 | 1.05 | | | | | | |
| 7 | 133.2 | .192 | 58.9 | .514 | 2.22 | .704 | .455 | 1.29 | | | | | |
| 8 | .109 | .031 | .742 | .166 | 1.42 | .235 | .789 | .450 | 1.37 | | | | |
| 9 | 174.5 | .222 | 77.8 | .559 | 3.06 | .643 | .645 | 1.18 | .900 | 1.42 | | | |
| 10 | .019 | .046 | .872 | .199 | 1.56 | .197 | .743 | .214 | 1.19 | .546 | 3.09 | | |
| 11 | 182.4 | .150 | 81.6 | .510 | 3.22 | .602 | .748 | .960 | 1.11 | 1.25 | .136 | 5.92 | |
| 12 | .138 | .016 | 1.01 | .230 | 1.68 | .190 | .718 | .193 | 1.17 | .622 | 2.58 | .615 | .826 |

uncertainty of an adjusted term is in fact due to the aliasing by the uncertainty of an arbitrarily selected unadjusted term.

The results of this strategy are displayed in both Figure 3 and Table 10 as percentage aliasing of the estimated uncertainty. One would intuitively expect that with such a dense and global distribution of data as obtained by GRAVSAT/GEOPAUSE, the aliasing would be negligible. It is seen, however, that even with such a good distribution of data the aliasing problem is quite severe.

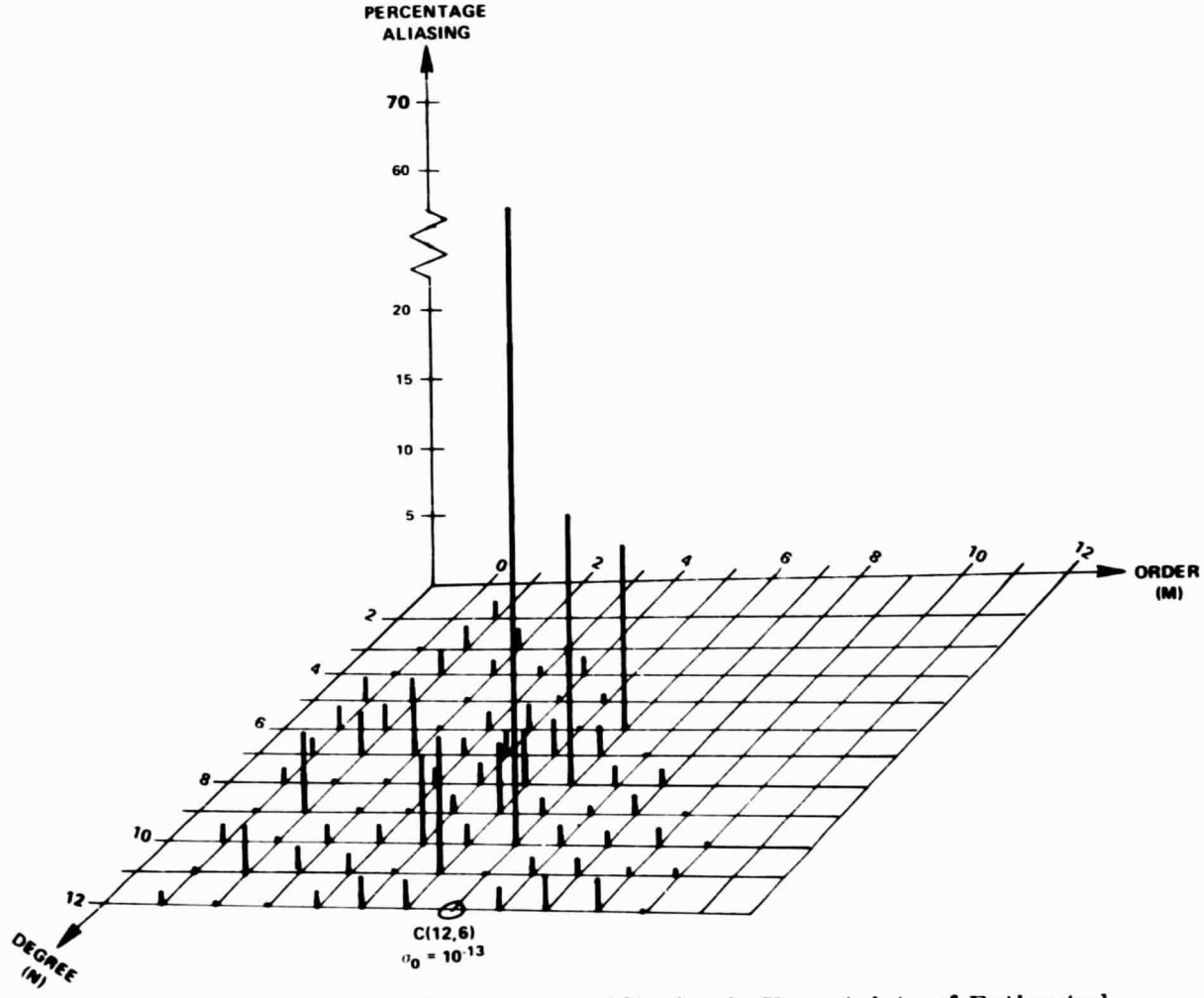


Figure 3. Histogram of Percentage Aliasing in Uncertainty of Estimated Cosine Coefficients Due To Unestimated Uncertainty of C(12, 6)

Table 10

**Percentage Aliasing in Uncertainty of Estimated Cosine Coefficients Due to Unestimated Uncertainty of C(12, 6)**

| Degree (N) \ Order (M) | 0 | 1 | 2 | 3 | 4 | 5 | 6 | 7 | 8 | 9 | 10 | 11 | 12 |
|---|---|---|---|---|---|---|---|---|---|---|---|---|---|
| 2 | .01 | .53 | .14 | | | | | | | | | | |
| 3 | .08 | 1.3 | .86 | .20 | | | | | | | | | |
| 4 | .02 | 2.1 | .47 | .43 | 1.6 | | | | | | | | |
| 5 | .62 | 1.9 | .08 | .26 | .24 | .63 | | | | | | | |
| 6 | .13 | 2.3 | .10 | .73 | 2.1 | .01 | 13.4 | | | | | | |
| 7 | .64 | 3.0 | 3.1 | .71 | 1.8 | 2.4 | 2.0 | .17 | | | | | |
| 8 | .72 | .29 | .27 | .59 | 1.1 | 3.8 | 19.9 | .79 | 1.2 | | | | |
| 9 | .08 | 6.3 | .25 | .18 | 1.1 | 5.3 | 1.1 | .55 | 1.8 | .40 | | | |
| 10 | .63 | .07 | .45 | 1.2 | 7.0 | 1.5 | 71.8 | .94 | .98 | 1.2 | .14 | | |
| 11 | .10 | 3.8 | 1.4 | .93 | .25 | 8.1 | .26 | .71 | 1.2 | .54 | .53 | .17 | |
| 12 | .34 | .13 | .16 | .57 | 2.3 | 1.7 | $^{0}$ $10^{-13}$ | .95 | 2.3 | 2.6 | .12 | .13 | .11 |

The unadjusted error of C(12, 6) is seen to alias the estimated uncertainty of all terms to some degree. The uncertainties of seven of these terms: C(6, 6), C(8, 6), C(9, 1), C(9, 5), C(10, 4), C(10, 6), and C(11, 5) experience the greatest impact with percentage aliasing ranging from 5 through 72%. The uncertainty for C(10, 6) stands out with the highest percentage aliasing of 72%. The uncertainties of all the remaining terms experience an aliasing effect below 5%.

## CONCLUSIONS

This report has described a covariance analysis of the GRAVSAT/GEOPAUSE mission in which the uncertainties of approximately 200 parameters were simultaneously estimated from the range sum rate data between these two satellites. The adjusted GRAVSAT epoch state errors are seen to be sensitive to the amount of data whereas the GEOPAUSE errors remain relatively insensitive. The actual magnitude of these errors indicate that data from the high GEOPAUSE spacecraft to a lower satellite can successfully be processed to estimate both orbits. In addition RSS position errors ranging from 60 to 20 cm, depending upon the amount of data, can also be extracted from such data. These accuracy levels represent improvements over the present 8.5m RSS accuracy level. The uncertainties of the geopotential field to (12, 12) were recovered to an accuracy one to two orders of magnitude superior to present estimates regardless of the amount of data. Consequently, if geopotential recovery is of prime interest, 3 days of tracking suffices. Geopotential aliasing is the degrading influence upon the uncertainties of estimated parameters due to the errors in the unestimated quantities. An alias map for an arbitrarily selected term, C(5, 2), revealed that the uncertainties of odd degree zonals contribute the maximum aliasing to the uncertainty of that term. The percentage aliasing in the estimated uncertainties of coefficients due to the error of a centrally located term of high degree and order term, C(12, 6), was also determined. The estimated uncertainties of most terms contained negligible, i.e. less than 5%, aliasing. However seven terms, ranging from degree 6 through 11, contained significantly higher aliasing.

REFERENCES


1. NASA, Earth and Ocean Physics Applications Program, Volume II, Rationale and Program Plans, September 1972.

2. Fairchild Industries Incorporated, Earth Harmonics Satellite Study, 854-FR-403-001.

3. D. Koch, P. Argentiero, W. D. Kahn, Long and Short Arc Altitude Determination for GEOS-C, GSFC Report X-591-73-368, November 1973.

4. Fairchild Industries Incorporated, Geopause Satellite Study, 854-FR-402-001, October 1971.

5. J. Siry, A Geopause Satellite System Concept, GSFC Report X-550-71-503, April 1971.

6. D. Koch, P. Argentiero, Simulation of the GRAVSAT/GEOPAUSE Mission, GSFC Report X-932-74-288, August 1974.

7. F. J. Lerch, et al, Goddard Earth Models (5 and 6), GSFC Report X-921-74-145, December 1974.

8. P. Argentiero, R. Garza-Robles, On Estimating Gravity Anomalies from Gradiometer Data, GSFC Report X-932-74-286, September 1974.

9. J. J. Lynn, J. G. Hartwell and R. S. Nankervis. "Network Analysis Program, NAP-3, Mathematical Analysis Documentation." DBA Systems, Inc. June 1, 1970.

10. R. Garza-Robles, S. Guion, T. Lewis and D. Lynn. "Network Analysis Program, NAP-3, Program Analysis Documentation." DBA Systems, Inc. June 1, 1970.

11. Old Dominion Systems, Inc., "User's Guide to Data Preparation, Navigation Analysis Program (NAP 3.1)," April 1974.

12. J. J. Lynn. NAPCOV Program Documentation." Old Dominion Systems, Inc. November 1973 (revised May 1, 1974).